JCTC Journal of Chemical Theory and Computation

Computational Analysis of the Mechanism and Thermodynamics of Inhibition of Phosphodiesterase 5A by Synthetic Ligands

Bojan Zagrovic* and Wilfred F. van Gunsteren

Laboratory of Physical Chemistry, ETH, Zürich, CH-8093, Switzerland

Received October 30, 2006

Abstract: Phosphodiesterases are a large class of enzymes mediating a number of physiological processes ranging from immune response to platelet aggregation to cardiac and smooth muscle relaxation. In particular, phosphodiesterase 5 (PDE5) plays an important role in mediating sexual arousal, and it is the central molecular target in treatments of erectile dysfunction. In this study, we look at the mechanism and thermodynamics of the binding of selective inhibitors sildenafil (Viagra) and vardenafil (Levitra) to PDE5 using molecular dynamics simulations. Our simulations of PDE5 with and without sildenafil suggest a binding mechanism in which two loops surrounding the binding pocket of the enzyme (H loop, residues 660−683, and M loop, 787−812) execute sizable conformational changes (∼1 nm), clamping the ligand in the pocket. Also, we note significant changes in the coordination pattern of the divalent ions in the active site of the enzyme, as well as marked changes in the collective motions of the enzyme when the ligand is bound. Using the thermodynamic integration approach we calculate the relative free energies of binding of sildenafil, vardenafil, and demethyl-vardenafil, providing a test of the quality of the force field and the ligand parametrization used. Finally, using the single-step perturbation (SSP) technique, we calculate the relative binding free energies of these three ligands as well. In particular, we focus on critical evaluation of the SSP technique and examine the effects of computational parallelization on the efficiency of the technique. As a technical improvement, we demonstrate that an ensemble of relatively short SSP trajectories (10 × 0.5 ns) markedly outperforms a single trajectory of the same total length (1 × 5 ns) when it comes to sampling efficiency, resulting in significant real-time savings.

Introduction

Phosphodiesterases are a large family of enzymes involved in hydrolyzing second messengers cyclic guanosine monophosphate (cGMP) and cyclic adenosine monophosphate (cAMP).[1,2] These two second messengers, produced by enzymes guanylyl and adenylyl cyclase, are key components in a number of different signal transduction cascades providing a link between the activity of extracellular receptors such as the G-protein coupled receptors and downstream intracellular effectors such as different kinases and phosphatases. By decreasing the cellular levels of cGMP and cAMP, phosphodiesterases regulate a multitude of physiological processes including smooth and cardiac muscle relaxation, platelet aggregation, apoptosis, and vision.[3]

There are in total 11 different classes of phosphodiesterases, each class involved in regulating a particular set of physiological functions.[4] Phosphodiesterase 5 (PDE5; Figure 1a), in particular, has been shown to play an important role in mediating sexual response.[5] More specifically, this enzyme is a negative regulator of the signal transduction cascade leading to the relaxation of corpus cavernosum tissue and subsequent penile erection. Inhibition of PDE5 is

* Corresponding author phone: 0041-44-632-5504; e-mail: zagrovic@igc.phys.chem.ethz.ch and igc-sec@igc.phys.chem.ethz.ch.

10.1021/ct600322d CCC: $37.00 © 2007 American Chemical Society
Published on Web 12/19/2006

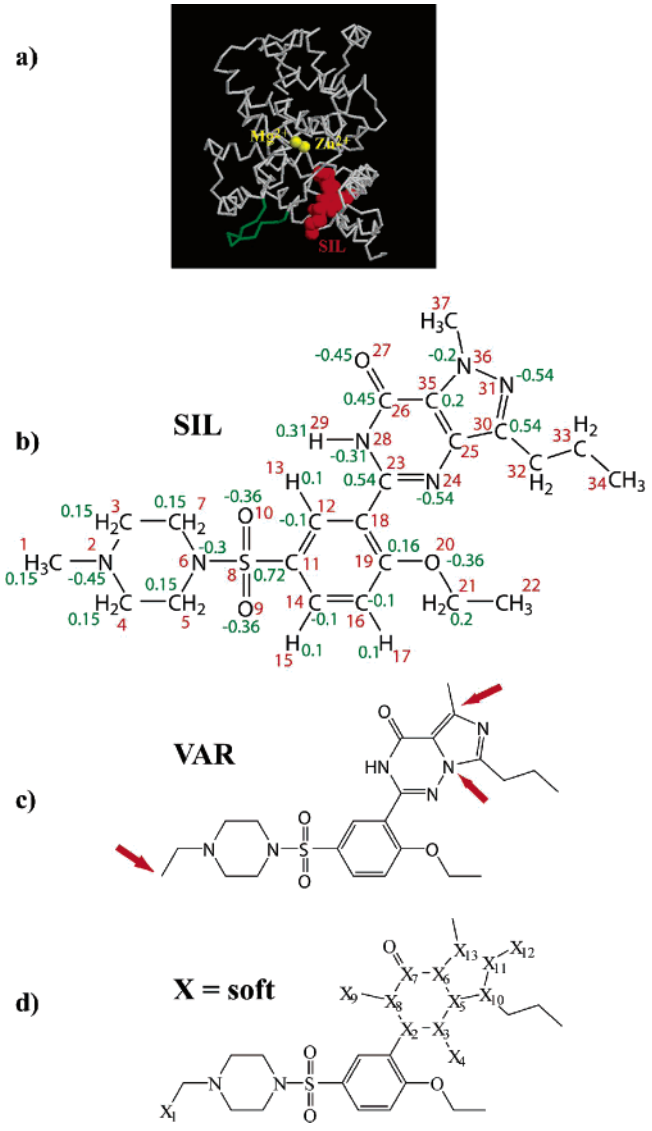

Figure 1. (a) X-ray structure of phosphodiesterase 5A (PDB code: 1UDT) with bound sildenafil (shown in red). The loop that was added (residues 665−675) is shown in green. The catalytically important divalent ions are shown in yellow. (b) Structure of sildenafil with atom numbers (red) and partial charges (green) from our parametrization. Atoms with no charges indicated have zero charge. (c) Structure of vardenafil. Points where it differs from sildenafil are labeled with arrows. (d) Structure of the soft reference state for the SSP technique. Soft atoms are depicted with X.

therefore a natural target in treatments of erectile dysfunction disorder, and several potent synthetic inhibitors of the enzyme have been developed.[6,7] These include the widely used sildenafil (Viagra), vardenafil (Levitra), and tardenafil (Cialis). While these ligands have proved to be very successful, significant efforts have been directed toward improving their pharmacological properties, in particular, decreasing cross-reactivity with other phosphodiesterase types. Namely, some of the side effects of using these drugs, including blurry vision and skin rash, can be attributed to nonselective inhibition of phosphodiesterases not involved in mediating sexual response such as phosphodiesterases 4B and 6.[5]

When it comes to the mechanism of binding of natural ligands as well as synthetic inhibitors to phosphodiesterases, significant progress has been made by detailed X-ray crystallographic analyses of different phosphodiesterase types.[6,8,9] In general, phosphodiesterase ligands bind in a deep, hydrophobic binding pocket, which penetrates all the way to a small water-filled cavity in the very core of the enzyme. This cavity houses two divalent ions, in most cases, magnesium and zinc, which take part in the catalytic stage of the hydrolysis reaction. Regarding the binding of ligands, two well-defined structural features of phosphodiesterases, common to all 11 classes of the enzyme, have been delineated.[6,8] First, a conserved glutamine residue forms a pair of strong bidentate hydrogen bonds with the purine moiety in cGMP, cAMP, and other structurally similar ligands, including sildenafil and vardenafil ("glutamine switch").[8] Second, a conserved valine on one side and an invariant aromatic residue on the other side sandwich the purine ring of the ligand in a fixed orientation with respect to the central cavity ("hydrophobic clamp").[6]

While X-ray analyses have taught us a lot about the mode of binding of different ligands to phosphodiesterases, they provide only an averaged, static picture of the process. Motivated by this, we have undertaken a computational analysis of PDE5A and its ligands sildenafil and vardenafil (Figure 1). By simulating in explicit solvent the enzyme in the presence and in the absence of sildenafil, we have obtained an atomistic picture of the dynamics and the structural mechanism of binding. Our simulations suggest a binding mechanism in which two particular loops surrounding the binding pocket of the enzyme (residues 660−683 and 787−812) undergo sizable conformational changes (∼1 nm), clamping the ligand in the pocket. Second, we observe significant changes in the coordination pattern of the divalent ions in the active site of the enzyme in the presence of a ligand. Finally, we note marked changes in the collective motions of the enzyme when the ligand is bound.

Using computational approaches, we have also analyzed the thermodynamics of ligand binding to PDE5A. Employing the thermodynamic integration technique, we have calculated the relative free energies of binding of sildenafil, vardenafil, and vardenafil with no extra methyl group attached to the piperazine moiety (demethyl-vardenafil).[10] Qualitative rank-order agreement between the calculated and experimental values testified about the adequacy of the force field used and motivated further calculations using the single-step perturbation technique (SSP).[11−13] In its traditional implementation, the SSP technique entails running two trajectories of a carefully chosen soft-core reference ligand, one in the binding pocket of a protein and another one free in solution. From these two trajectories, one should, in principle, be able to derive relative free energies of binding for a large set of real ligands. In addition to a good design of the reference state, the principal challenge for successful application of the SSP technique is adequate sampling of the phase space belonging to the reference state and, indirectly, to all the real ligands whose relative free energies of binding one is interested in.[13] As a consequence, motivation exists to try to improve the sampling of the low-energy states visited in

SSP simulations, while still retaining the method's greatest advantage, computational efficiency. Stimulated by the widespread presence of computer clusters of loosely coupled processors, we have here examined the potential of brute-force parallelization of the SSP approach and its effects on the degree of sampling that can be achieved. Here, by "brute-force parallelization" we mean simple simulation of multiple trajectories of the reference state on a series of fully independent processors. We show how simulating an ensemble of relatively short trajectories results in much better coverage of the configuration space of the protein−ligand complex compared with one single, long trajectory of the same total length. Also, the ensemble approach is shown to be significantly more successful in selecting low-energy states, which dominate thermodynamic averages when it comes to calculation of the relative binding free energies. Most importantly, these improvements are obtained with a linear speedup in the wall-clock time used, resulting in large real-time savings. For example, generating 10 0.5 ns trajectories of the soft state in the protein took only 5 days on a Pentium III cluster, while generating one 5 ns trajectory took approximately 50 days.

Materials and Methods

All simulations were performed using the GROMOS simulation package.[14] The initial structure of PDE5A (324 residues) with sildenafil bound[9] was taken from the Protein Data Bank (code: 1UDT) and was placed in a pre-equilibrated truncated octahedron box filled with SPC[15] water molecules (box size 9 nm, for a total of 10 619 water molecules). Parts of the H loop (residues 665−675; throughout this paper, the amino acid numbering corresponds to the original numbering in the 1UDT structure) missing in the 1UDT structure because of disorder were modeled-in using the Modloop routine in the software package Modeller.[16,17] In all simulations, an equilibration scheme was carried out, which included raising the simulation temperature from 60 to 300 K while simultaneously decreasing the position restraint coupling constant from 25 000 to 0 kJ/mol in five equidistant steps for both the temperature and coupling constant. At each equilibration step, a short 20 ps simulation at a constant volume was carried out. This was followed by another 20 ps at 300 K and 1 atm of pressure and a subsequent production run. Constant temperature and pressure were maintained by a Berendsen thermostat (coupling time of 0.1 ps) and barostat (coupling time 0.5 ps), respectively.[14,18] All simulations were carried out using the GROMOS 45A3 force field,[19] using periodic boundary conditions. The atom numbers and partial charges for the sildenafil ligand are given in Figure 1b. The structure of vardenafil is given in Figure 1c with differences with respect to sildenafil marked with arrows. Complete GROMOS building blocks for sildenafil and vardenafil are given in the Supporting Information. Electrostatics were treated using the reaction field approach and the triple-range cutoff scheme, with cutoffs of 0.8 and 1.4 nm, and a dielectric permittivity of 61. The pair list was updated every five steps. The equations of motion were integrated using the leapfrog scheme and a step size of 2 fs. All bonds were constrained using the SHAKE algorithm[20] with a tolerance of 0.0001. Initial velocities were taken from the Maxwell−Boltzmann distribution at 300 K.

A total of 10 3-ns-long trajectories were simulated each for free PDE5A and PDE5A with sildenafil bound. The starting structure of the free enzyme was generated from the 1UDT structure by removing the ligand. Each of the 10 trajectories in the two cases was initiated with different starting velocities chosen from the Maxwell−Boltzmann distribution at 300 K. For both setups, the 10 trajectories were started from the same starting structure after the equilibration period as described above.

Thermodynamic integration was carried out using the standard λ-dependent approach, with 26 λ points spaced equidistantly between 0 and 1.[21] At each λ point, the system was simulated for 500 ps, but the first 100 ps were considered the equilibration period and were not used for calculating thermodynamic averages. To prevent instabilities, the soft-core approach was followed[22,23] with $\alpha_{ij}^{LJ} = 0.5$. Electrostatic interactions were treated using $\alpha_{ij}^{C} = 0.5$ nm^2. The area underneath the $\langle \partial H/\partial\lambda \rangle$ curves was calculated using trapezoidal integration. The statistical error at each λ point was estimated using the block averaging technique with blocks of different sizes.[24]

Binding free energy differences were also calculated using the SSP technique.[11−13] Here, we outline the basics of the technique and its present implementation: for more details, the reader is referred to one of the existing references.[11−13,25−29] The free energy difference between thermodynamic states A and R can be calculated using the perturbation formula:[30]

$$\Delta G_{AR} = -k_B T \ln\langle e^{-(E_A - E_R)/k_B T} \rangle_R \quad (1)$$

where E_A and E_R are the potential energies of the system in states A and R, respectively, k_B is the Boltzmann constant, and T is the temperature. The ensemble average, denoted by the brackets, is carried out over all the configurations of state R that can be generated in a simulation. In a typical application, states A and R, for example, represent two different ligands bound to the same receptor. In the SSP approach, the state R is a so-called reference state, a potentially unphysical ligand whose configuration space, as sampled in a simulation, exhibits significant overlap with configuration spaces of several different ligands whose relative free energies of binding one is interested in calculating.[13] Post analysis of the molecular dynamics simulations of the reference ligand free in solution and bound to a receptor allows one then to calculate the relative free energy of binding between a real ligand and the reference ligand by using eq 1. By doing this for two different ligands, one can obtain their relative free energy of binding using the following identity:

$$\Delta\Delta G_{BA} = \Delta G_{BR}(\text{bound}) - \Delta G_{BR}(\text{free}) - \Delta G_{AR}(\text{bound}) + \Delta G_{AR}(\text{free}) \quad (2)$$

The chief advantage of the SSP technique is that it allows one to, in principle, calculate relative free energies of binding of a large series of real ligands from a pair of simulations of the reference ligand. In order to expedite sampling and ensure that the sampled configurations of the reference state exhibit

significant overlap with configuration spaces of a number of real ligands, the nonbonded interaction function of the atoms in the reference ligand is typically made soft by removing the singularity at the origin. More precisely, the Lennard-Jones interaction involving atoms of choice is modified in such a way that there is a finite probability that two atoms fully overlap in space. This modification is applied to all those atoms which differ between different real ligands of interest.[22]

The atoms treated as soft are depicted with X in Figure 1d. In our implementation, the softness parameter α_{ij}^{LJ} is set to 1.51 for all soft atoms, while for electrostatic interaction, α_{ij}^{C} is set to 1.11 nm^2 for charged soft atoms.[13] The GROMOS nonbonded interaction atom types for these atoms in the soft state are those of the equivalent atoms in sildenafil. The same goes for bonded interactions. The only exceptions are the soft atoms X4 and X12 (Figure 7a), which were treated as hydrogen atoms (GROMOS nonbonded interaction atom type 18). Other GROMOS force-field types regarding these two atoms are as follows: bonds, 24−X4 and 31−X12 bond type 2; angles, 23−24−X4 and 25−24−X4 bond-angle type 24 and 30−31−X12 and 36−31−X12 bond-angle type 35; improper dihedrals, 24−23−X4−25 and 31−30−X12−36 harmonic dihedral type 1 (here, atom numbers refer to Figure 1b for the real atoms and Figure 1d for the soft atoms). Most soft atoms were assigned no charge except X6 (0.1 *e*), X7 (0.25 *e*), and X8 (0.1 *e*) to balance the negative charge on the nearby carbonyl oxygen. The simulation of the reference ligand in water was carried out in a cubic box with sides of 3.5 nm containing a total of 1585 water molecules. The simulations of PDE5A bound to the reference ligand were carried out in a truncated octahedron box with sides of 9.0 nm containing a total of 10 619 water molecules. For both the reference ligand in water and reference ligand bound to the protein, 10 independent 0.5-ns-long trajectories were run, each initiated from the same pre-equilibrated configuration with different velocity assignments. The pre-equilibration was carried out with the real sildenafil ligand as described above, followed by a 10 ps equilibration with soft parameters at 1 atm of constant pressure and subsequent production runs. In addition, one of the 10 trajectories in both cases was extended to a total length of 5 ns. In all cases, structures were saved for analysis every 0.2 ps.

Results

Structural Analysis and Mechanism of Binding. To enhance the sampling of the configuration space accessible to the molecule, we have run 10 independent 3-ns-long simulations of PDE5A without and with sildenafil bound, each simulation initiated with different velocities. The simulations are stable with respect to both the secondary and tertiary structure of the protein as well as the position of the ligand in the binding pocket. Time traces of the backbone atom-positional root-mean-square deviation (RMSD) from the experimental X-ray structure for the entire protein are shown in Figure 2a for both the unliganded and liganded PDE5A. In both cases, the average RMSD stabilizes around 0.3 nm, with only one out of 10 trajectories in each setup exceeding 0.4 nm at any point. Interestingly, the variance of the RMSD curves is appreciably greater in the presence of the ligand than without it. This fact is also mirrored in the behavior of the two divalent ions, zinc and magnesium, located in the central cavity of the protein. In the presence of sildenafil, not only does the separation between these two ions increase by approximately 0.1 nm but so does the degree of variability in this separation between different trajectories in the ensemble (Figure 2b). Visual analysis of the simulated trajectories reveals that the reason for this lies in the significant change in the coordination of the divalent ions when sildenafil is bound. In the absence of the ligand, the negatively charged side chains of residues Asp 654 and Asp 764 equally coordinate the two ions (Figure 2c on the left), resulting in a stable configuration with small fluctuations in the separation between the ions. In the presence of the ligand, these two residues provide symmetric coordination for the Zn^{2+} ion, while the Mg^{2+} ion is solely coordinated by the water molecules in the cavity (Figure 2c). This allows for its larger mobility and, subsequently, larger separation from the Zn^{2+} ion and larger overall variance of the distance between them.

What stabilizes sildenafil in the binding pocket? We have analyzed both principal contributions to sildenafil binding indicated in the literature, that is, "hydrophobic clamp" and "glutamine switch".[6,8] Both of these proposed mechanisms gain support from our simulations. In Figure 3a, we show the distribution of the angle between the planes of the purine ring in sildenafil and the phenyl ring of Phe 820, key participants in the "hydrophobic clamp" mechanism.[6] These two moieties remain largely parallel with each other, resulting in a stabilizing stacking interaction. Val 782, implicated in stabilizing sildenafil's purine ring in its position, remains in close contact with the ligand throughout the simulations (Figure 3b). Finally, if one analyzes the conserved Gln817, its amide group forms two hydrogen bonds with the purine group of sildenafil 40% of the time, at least one hydrogen bond 93% of the time, and no hydrogen bonds only 7% of the time. Such strong hydrogen bonding is an essential component of the "glutamine switch" mechanism,[8] and it is evident in our simulations as well.

In addition to the previously described "glutamine switch" and "hydrophobic clamp", our simulations suggest a third, novel contribution to ligand stabilization by phosphodiesterases, which we now term "loop clamp". In the original 1UDT X-ray structure of the molecule, parts of the H loop (residues 665−675) were missing in the density, supposedly because of their high mobility, and were modeled-in for our simulations. It is precisely this H loop, together with an opposing M loop (residues 787−812), which participates in a sizable conformational change upon binding of sildenafil (Figure 4). As the ligand binds, the H loop moves toward the M loop by more than 0.7 nm on average, with many configurations exhibiting changes in excess of 1 nm. In effect, the two loops close down on the ligand clamping it in its position. In Figure 4a, we show the average time trace of the distance between residues His 670 and Asn 798: as is evident, these two residues come closer by on average 0.6−0.8 nm in the presence of the ligand. This fact is even more clearly illustrated if one looks at the distribution of

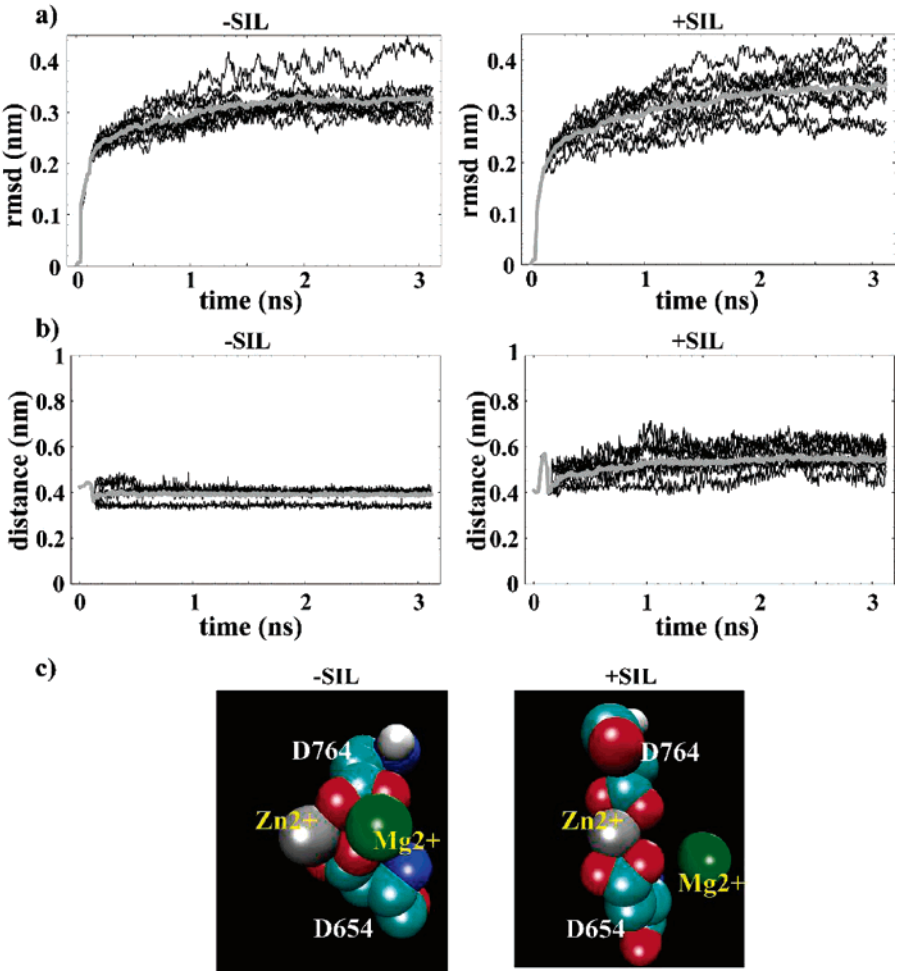

Figure 2. (a) Backbone atom-positional RMSD from the experimental X-ray structure for 10 trajectories without (left) and with (right) sildenafil bound. Backbone atoms were used for both rotational fitting and RMSD calculation. (b) Distance between two divalent ions in the core of the protein for the simulations without (left) and with (right) sildenafil bound. Average traces in a and b are shown in gray. (c) Coordination of the Zn^{2+} and Mg^{2+} ions in the active site of the enzyme without and with sildenafil bound. In the absence of sildenafil, the carboxyl groups of the residues Asp 654 and Asp 764 coordinate both ions equally. With sildenafil bound, these two residues exclusively coordinate the Zn^{2+} ion, while the Mg^{2+} ion moves more freely, being coordinated by water molecules only. This explains the difference in the fluctuations in the distance between the two ions in the two states (Figure 2b). Color code: oxygen, red; zinc ion, gray; magnesium ion, green; nitrogen, blue; carbon, cyan.

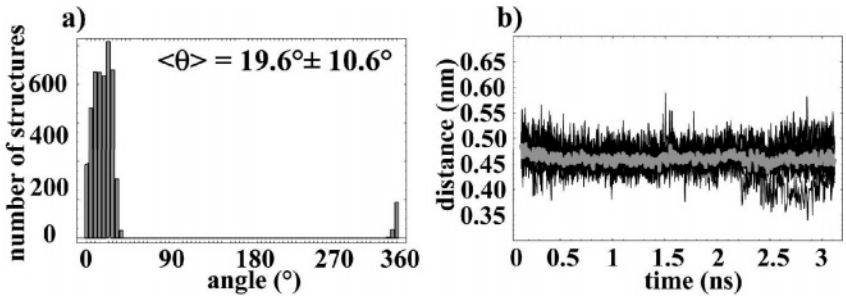

Figure 3. (a) Distribution of the angle between the plane of the purine ring of sildenafil and the phenyl ring of Phe 820. (b) Distance between CB in Val 782 and atom 35 in sildenafil over time for the 10 trajectories with sildenafil bound. The average trace is shown in gray.

this distance over the last 1.5 ns in all 10 trajectories (Figure 4b). The clamping motion of the two loops is exemplified in Figure 4c for two representative members of the ensembles without and with sildenafil bound.

Analysis of the atom-positional root-mean-square fluctuations (RMSF) of the protein around the average configuration (Figure 5a) reveals significant collective changes in the dynamics of the protein in the presence of the ligand compared to a situation with no ligand bound. Looking at the difference in RMSF when the ligand is bound versus when it is not (Figure 5b,c), calculated over the last 1.5 ns of the trajectories, one sees distinct contiguous regions of the protein whose fluctuations collectively increase, that is, decrease when the ligand is bound. In particular, fluctuations

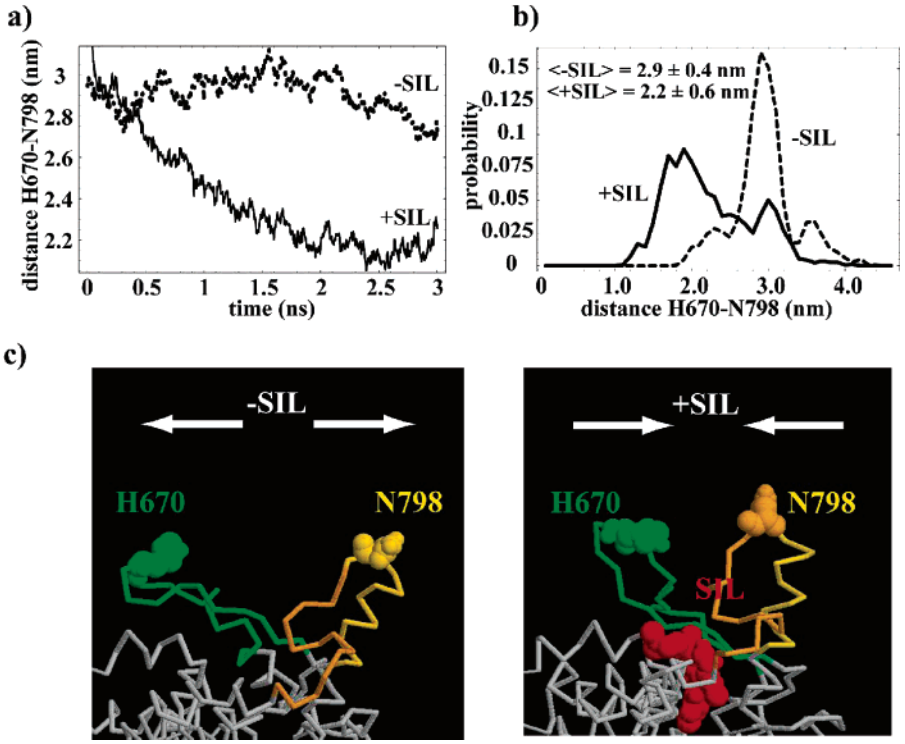

Figure 4. (a) Time traces of the Cα−Cα distance between residues His 670 and Gln 798 without and with sildenafil bound, averaged over the 10 3 ns trajectories in the two states. (b) Distributions of the Cα−Cα distance between residues His 670 and Gln 798 without and with sildenafil bound, for both ensembles over the last 1.5 ns of simulation. Distributions were binned using 0.1 nm bins. (c) Two representative structures from the simulations without and with sildenafil bound. H and M loops are outlined in green and yellow, respectively. Residues His 670 and Gln 798 are shown in an explicit van der Waals representation.

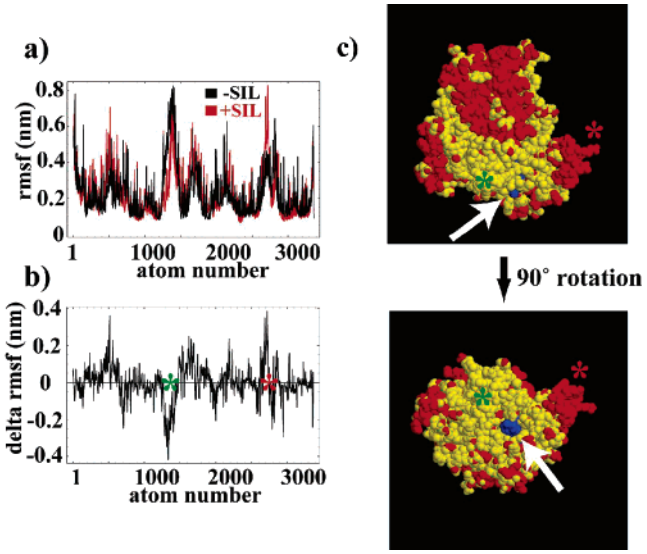

Figure 5. (a) Atom-positional root-mean-square fluctuations (RMSF) calculated with respect to the average structure without (black) and with (red) sildenafil bound. (b) Difference between the RMSF values with and without sildenafil bound, rmsf(+SIL) − rmsf(−SIL). (c) Values from b mapped onto the structure of PDE5A (yellow, RMSF decreases with sildenafil bound; red, RMSF increases with sildenafil bound). Position of the sildenafil binding pocket is indicated with an arrow. In b and c, locations of the H and M loops are marked with green and red stars, respectively.

of the protein around the binding pocket decrease in the presence of the ligand, while the diametrically opposite apical region of the enzyme largely increases in motion (Figure 5c). The behavior of the loops surrounding the binding pocket is particularly noteworthy. The M loop increases in its fluctuations despite getting closer to the H loop. On the other hand, the H loop, which undergoes a much larger relative motion, decreases in fluctuations participating more strongly in relative terms in clamping the ligand in the binding pocket.

Thermodynamics. *Thermodynamic Integration.* Standard λ-dependent thermodynamic integration[21] was carried out to calculate relative free energies of binding of sildenafil and vardenafil. The two molecules differ by the type (N versus C) of only two atoms (25 and 36) of the purine ring, but, in addition, vardenafil has an extra methyl group attached to the piperazine ring (Figure 1b,c). The latter has been shown to make no significant contribution when it comes to the free energy of binding: vardenafil with no methyl group (demethyl-vardenafil) still binds to PDE5A about 10 times more potently than sildenafil.[10] Average $\partial H/\partial\lambda$ curves for the sildenafil-to-vardenafil conversion are shown in Figure 6a (ligand in water and in the binding pocket). Numerical integration of these curves yields a relative free energy of binding of −8.0 kJ/mol, which is in agreement with experimental results. Measurements of the IC_{50} values for PDE5A give a range of 1−7 nM for sildenafil[31,32] and 0.17 nM for vardenafil.[10] This corresponds to a free energy difference of anywhere between −9.3 and −4.4 kJ/mol. Measurements of K_D values, which are a better indication of affinity, yield a range of 8.3−13 nM for sildenafil[10] and 1 nM for vardenafil.[33] This equals a range from −5.8 to −5.3 kJ/mol, when it comes to free energy differences.

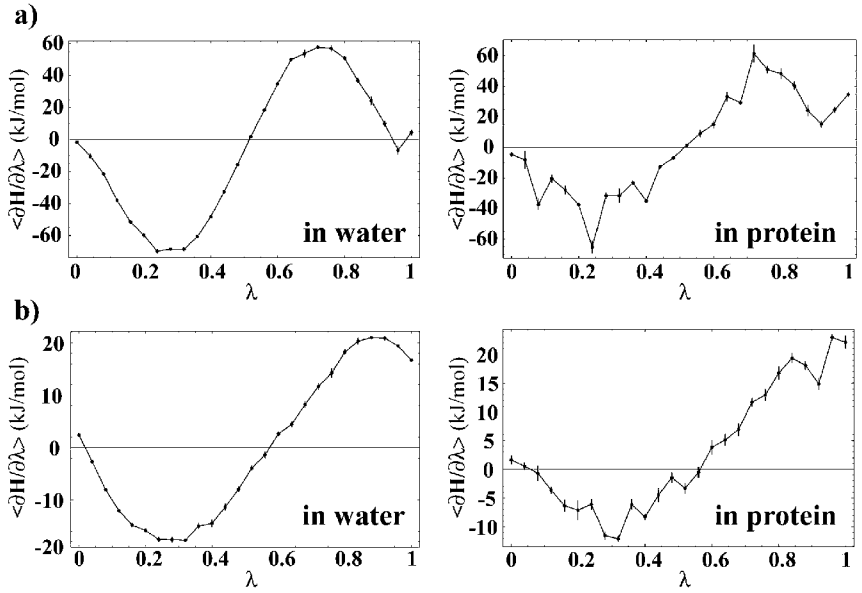

Figure 6. Average thermodynamic integration $\langle \partial H/\partial \lambda \rangle$ curves for simulations of the free ligand ("in water") or ligand bound to the protein ("in protein") for (a) vardenafil ($\lambda = 0$) to sildenafil ($\lambda = 1$) conversion and (b) vardenafil ($\lambda = 0$) to demethyl-vardenafil ($\lambda = 1$) conversion. Vertical bars refer to the statistical error at each λ value (see Methods for details).

As a control, we have also performed another 26-point λ-dependent thermodynamic integration for the conversion from vardenafil to demethyl-vardenafil.[10] Average $\partial H/\partial \lambda$ curves for this conversion are shown in Figure 6b: we calculate a relative free energy of binding of 3.4 kJ/mol. The range of experimental values for this free energy difference is anywhere between -2.1 (based on K_D values) and -0.5 kJ/mol (based on IC_{50} values), indicating essentially no significant effect of the piperazine methyl group on the binding. While the simulations do not ideally match the experimental data, they still provide a qualitatively correct picture of binding: these results give us confidence in the force field used as well as in the parametrization of the two ligands.

Single Step Perturbation. In order to study the effects of computational parallelization in the context of SSP, we have first simulated 10 independent 0.5 ns trajectories of the reference ligand (Figure 1d) in the protein and another 10 free in solution, each trajectory being initiated from the same configuration, but with different velocity assignments. Second, we have extended one of the 10 short simulations of the soft reference ligand, chosen at random, to a total length of 5 ns, once in the protein and once free in solution. As shown in Figure 7a, the backbone atom-positional root-mean-square deviation for the entire protein from the experimental structure for both setups parallels to a large degree the results of our simulations with the real sildenafil ligand bound (Figure 2a). The RMSD in the case of the 5 ns simulation reaches about 0.3 nm on average, while in the case of the 0.5 ns trajectories, it remains around 0.25 nm with only one trajectory exceeding 0.35 nm at one point.

How does the sampling in the two cases compare? Equivalently, how diverse are the structures generated in the 5 ns trajectory as opposed to the ones coming from the composite ensemble consisting of the 10 0.5 ns trajectories? One way to assess this is shown in Figure 7b. We have

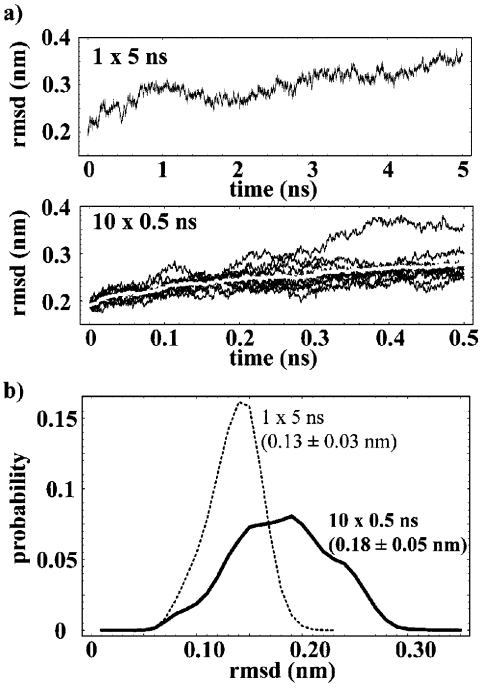

Figure 7. (a) Time traces of the backbone atom-positional RMSD from the experimental X-ray structure for the 5-ns-long trajectory and 10 0.5-ns-long trajectories with the soft ligand bound. The average trace for the ensemble is shown in gray. (b) Distributions of all-against-all atom-positional RMSD values for the structures from the 10 × 0.5 ns ensemble and the structures from the 1 × 5 ns trajectory. Only protein atoms within 0.5 nm from the nearest ligand atom were used for rotational fitting and RMSD calculation. The mean and standard deviation of each distribution is indicated. Distributions were binned using 0.01 nm bins.

calculated an all-against-all atom-positional RMSD matrix for 1000 structures, spaced every 5 ps, for each of the two ensembles, where for rotational fitting and RMSD calculation

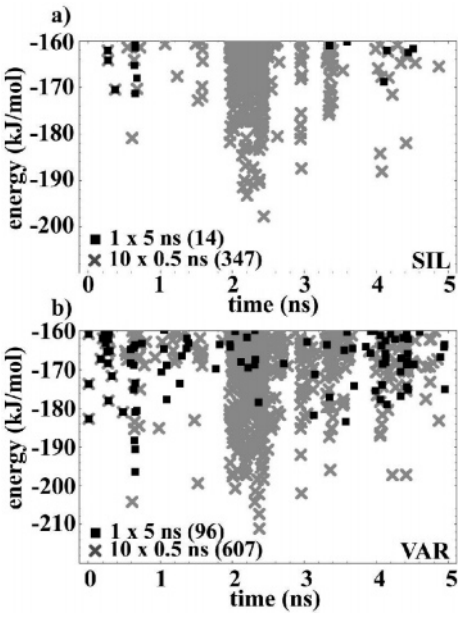

Figure 8. Low-lying energy configurations (<−160 kJ/mol) for an ensemble (10 × 0.5 ns, crosses) or a single trajectory (1 × 5 ns, boxes) for bound (a) sildenafil or (b) vardenafil. Energies are nonbonding energies for all the atoms that were soft in the reference state simulations. The number of individual configurations whose energy is less than −160 kJ/mol is indicated in the graphs. In the case of the 10 × 0.5 ns ensembles, trajectories were concatenated in post analysis to yield one 5-ns-long trajectory.

we have used only those atoms of the protein which are 0.5 nm or less away from the nearest atom of the bound ligand. Interactions between these atoms in the protein and the ligand are supposed to give the largest contribution to the final free energy of binding. In Figure 7b, we show the distribution of the RMSD values generated in this way: strikingly, even though one has used the same amount of processing time in the two cases, the ensemble approach with short trajectories yields a significantly greater diversity of structures according to the RMSD measure than does the single long trajectory. In particular, the average RMSD between the members of the single-trajectory ensemble is 0.13 ± 0.02 nm, while this number climbs to 0.18 ± 0.04 nm in the case of the multiple-trajectory ensemble.

How do the energies differ between the two setups? In Figure 8, we show total nonbonding energy values of the lowest-energy configurations coming from the two setups, calculated for the built-in sildenafil and vardenafil ligands. More precisely, energies were calculated for all the atoms that were simulated using the soft-core interaction, but after replacement by real-atom parameters, as required by a given real ligand. As can be seen, short parallel trajectories result in a significantly larger number of low-energy configurations compared to a long trajectory of the same overall length, and this is true for both ligands. For example, while the 5 ns trajectory results in 14 configurations of bound sildenafil with energy below −160 kJ/mol, this number rises to a total of 347 in the case of the 10 0.5 ps trajectories (Figure 8a). This ratio changes to 96 versus 607 configurations, respectively, in the case of vardenafil (Figure 8b). In general, the entire distribution of energy of the configurations coming from the ensemble of short trajectories is shifted toward lower energy values compared to the long trajectory (Figure 9b,d). However, this is true only for the simulations of the ligand in the binding site of the protein: parallelization results in no advantage when it comes to simulations of the ligand free in solution (Figure 9a,c). This is a direct manifestation of the fact that, in the allotted time, the single long trajectory manages to explore the majority of the relevant phase space volume available to the ligand free in solution. As the system behaves ergodically, there is then no difference between running a number of independent trajectories or just one long one. On the other hand, the barriers between low-energy conformations of the ligand are larger in the presence of the protein, which slows down the sampling and consequently makes the ensemble approach more advantageous. This advantage comes from the fact that, by choosing different starting velocities for the 0.5 ns replicas, one already from the start samples different regions of the phase space. As the barriers between these regions can be sizable, they do not get traversed in the course of the 5 ns trajectory, resulting in that case in exploring only a limited section of the phase space.

Finally, the advantage of the ensemble approach reflects itself in the cumulative curves depicting the buildup of the relative binding free energies of the ligands. Sharp, negative deflections in the ΔG_{AR} (relative free energy of the real ligands with respect to the soft state) curves are indicative of finding low-energy configurations that significantly contribute to the final ΔG_{AR} value. As is evident from Figure 10, there is an appreciably greater number of such configurations coming from the ensemble set as opposed to the single trajectory for both ligands. However, even more important is the fact that the final average relative free energy of binding is significantly more negative in the case of the ensemble approach: running several short trajectories manages to pick out low-energy configurations much more efficiently than does one single, long trajectory.

Discussion

Our observation of significant conformational changes in the H and M loops of PDE5A upon the binding of sildenafil is interesting as it represents a third, novel contribution to the stability of the ligand in the binding pocket, in addition to the previously described "glutamine switch"[8] and "hydrophobic clamp".[6] The two loops cover up the ligand in the binding pocket, clamping it in its position, and hence we term this feature of the enzyme the "loop clamp". Here, it should be emphasized that, in this clamping motion, the H loop undergoes a significantly greater motion compared to the M loop, which remains close to its average unbound position but starts fluctuating around it more significantly (Figure 5c). When our computational study was being initiated, there was no complete structure of the H loop available, and we resorted to modeling techniques to build it into the initial structure. As our study was already completed, a series of new X-ray structures of PDE5A appeared,[34] including, most importantly, structures of the enzyme with and without sildenafil bound, both with the H

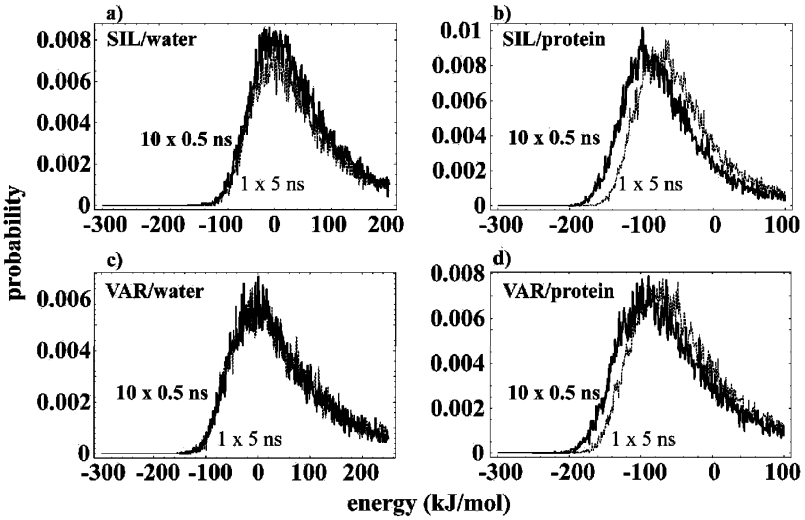

Figure 9. Distributions of nonbonding energies for an ensemble (10 × 0.5 ns, thick lines) or a single trajectory (1 × 5 ns, dashed thin line) for (a) sildenafil or (b) vardenafil in water (left) or in the protein (right). Energies are nonbonding energies for all the atoms that were soft in the reference state simulations. All distributions were binned in 1 kJ/mol bins.

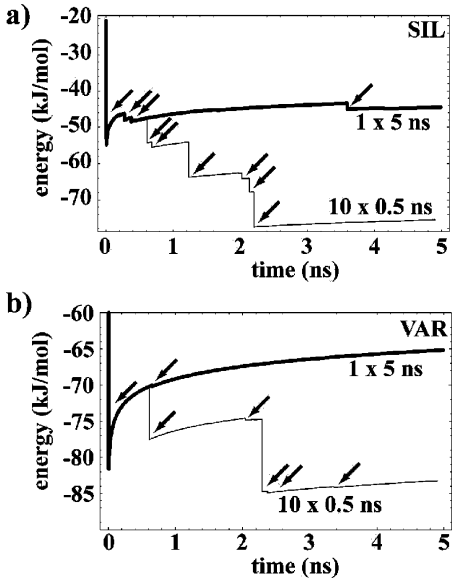

Figure 10. Development of the ensemble average value for ΔG_{AR} (relative free energy of a real ligand with respect to the soft ligand) for (a) sildenafil and (b) vardenafil. Configurations, which contribute significantly to the average, cause discontinuities in the graphs and are indicated by arrows. In the case of the 10 × 0.5 ns ensembles, trajectories were concatenated in post analysis to yield one 5-ns-long trajectory.

loop fully resolved. In this study, Ke and co-workers observed large-scale motions of the loop upon binding of the ligand, which are in many respects in good agreement with our observations. In their structures, the H loop executes an approximately 2 nm motion forming close van der Waals contacts with the piperazine moiety of sildenafil, resulting in almost complete burial of the ligand in the binding pocket. This is highly analogous to what we see, except that in our simulations the two dominant conformations of the H loop are slightly less apart (Figure 4b). Interestingly, Ke and co-workers also note small motions of the M loop toward the H loop, again analogous to what we see. Here, it should be mentioned that, even in the presence of the ligand, a small subset of our simulated structures remains in an unclamped position with H and M loops spread apart. In their measurements of the binding constant of sildenafil to PDE5A, Corbin and co-workers[33] observed two different dissociation constants for the ligand, a slow one and a fast one. It is possible that the fast and the slow dissociation constants reflect dissociation from a heterogeneous ensemble of structures, some of which have the loops spread apart and some of which have them clamped together. In the latter case, for dissociation to occur, the loops would first have to open up, resulting in a slower apparent dissociation rate.

Despite the improvements in sampling achieved through parallelization, the SSP results for the relative free energies of binding of vardenafil, sildenafil, and demethyl-vardenafil are at odds with the experimental findings as well as thermodynamic integration results. In Table 1, we summarize the relative free energies of binding and their components for vardenafil versus sildenafil and vardenafil versus demethyl-vardenafil. In both cases, the SSP results are both quantitatively and qualitatively at odds with the experimental results. While the experiment suggests the ordering of vardenafil, demethyl-vardenafil, and then sildenafil, going from the strongest to the weakest binder, the SSP results give an exactly opposite ordering, with sildenafil being the best binder. If one looks at the single 5 ns trajectory and calculates the free energy estimates over its first and second halves, one gets significantly different values for the ligand in the protein. This is a strong indication that the trajectory is not covering all of the relevant configurations in the time allotted. Interestingly, the first 2.5 ns of this trajectory yield a free energy difference for vardenafil and sildenafil (−3.6 kJ/mol) which is close to the experimentally determined value. This agreement, however, is purely fortuitous. In general, the free energies of the ligand in the protein are likely the ones causing the overall disagreement with experimental results: the convergence of the free energy values for the ligand in water is in general much better.

The fact that the thermodynamic integration results are in a much better agreement with experimental results suggests

Table 1. Free Energy Difference in Water and in the Protein for Vardenafil versus Sildenafil (var-sil) and Vardenafil versus Demethyl-Vardenafil (var-dmvar) Using the Single-Step Perturbation (SSP) Technique[a]

	water (kJ/mol)	protein (kJ/mol)	total (kJ/mol)
$\Delta\Delta G_{var-sil}$ (1×)	−18.3	−20.7	−2.4
$\Delta\Delta G_{var-sil}$ (1×, 0−2.5 ns)	−19.0	−22.6	−3.6
$\Delta\Delta G_{var-sil}$ (1×, 2.5−5 ns)	−16.0	−10.1	5.9
$\Delta\Delta G_{var-sil}$ (10×)	−18.0	−7.8	10.2
$\Delta\Delta G_{var-sil}$ (merged)	**−17.9**	**−7.8**	**10.1**
$\Delta\Delta G_{var-sil}$ (experiment)	**n/a**	**n/a**	**−9.3 to −4.4**
$\Delta\Delta G_{var-dmvar}$ (1×)	−4.1	−9.9	−5.8
$\Delta\Delta G_{var-dmvar}$ (1×, 0−2.5 ns)	−4.6	−11.9	−7.3
$\Delta\Delta G_{var-dmvar}$ (1×, 2.5−5 ns)	−2.3	0.7	3.0
$\Delta\Delta G_{var-dmvar}$ (10×)	−4.3	3.2	7.5
$\Delta\Delta G_{var-dmvar}$ (merged)	**4.3**	**3.2**	**7.5**
$\Delta\Delta G_{var-dmvar}$ (experiment)	**n/a**	**n/a**	**−2.1 to −0.5**

[a] The values are given for the single 5 ns trajectory (1×), the first and the last 2.5 ns of this trajectory (0−2.5 ns and 2.5−5 ns), a composite ensemble consisting of the 10 0.5 ns trajectories (10×), and another composite ensemble in which the 5 ns trajectory was merged with the 10 × 0.5 ns ensemble (merged). Experimental values were based on IC_{50} and K_D values (see text for details).

that the shortcomings of the SSP technique may not be attributed to the deficiencies of the force field used. Rather, the problems are likely to be traced to insufficient sampling as well as to the properties of the reference ligand employed. The reference ligand was designed with mostly neutrally charged soft atoms in the purine ring. The fact that the real ligands vardenafil and sildenafil possess significant partial charges in places where the reference ligand has none, and which are in key positions of opposite polarity, may cause the configurations sampled with the reference ligand to exhibit only little overlap with the configurational space of the real ligand, resulting in poor approximations of the relative binding free energy. This problem has been encountered before, and it represents one of the pressing challenges hindering the further development of the technique. Initially, our aim was to use the SSP technique to calculate the relative binding free energies for a series of different ligands of similar geometry, most of which have not even been synthesized or experimentally tested. This is the reason for using soft atoms in more positions than would be warranted just by the differences between the three ligands that we have analyzed here. However, the unsatisfying agreement with the experiment for these three ligands suggests that such attempts may be premature.

While the results of the SSP calculations may not be fully satisfactory, the demonstration of significant improvements in sampling obtained via brute force parallelization gives hope that further tests and improvements of the method could now be carried out more quickly and with better coverage of the phase space. SSP is essentially a thermodynamic technique, meaning that the exact trajectories of the soft state per se are of no particular interest. What matters is that these trajectories sample well the phase space available to ligands and receptors. In this sense, running multiple short trajectories should pose no problems. One could argue that, if one is interested in kinetics and mechanisms, having single trajectories that are long enough to capture conformational changes of interest, that is, barrier crossing events, may be of advantage. In the case of thermodynamics, using short trajectories should not be a problem, as long as they are long enough to sample well the local free energy minima. We hope that computational parallelization will lead to improvements of the SSP method itself, such that it can reach the levels of accuracy of the much more costly thermodynamic integration.

Acknowledgment. B.Z. acknowledges support from an EMBO postdoctoral fellowship. This work was financially supported by grants from the National Center of Competence in Research (NCCR) in Structural Biology and by grant number 200021-109227 of the Swiss National Science Foundation, which is gratefully acknowledged.

Supporting Information Available: GROMOS 45A3 building blocks for sildenafil and vardenafil are given. This information is available free of charge via the Internet at http://pubs.acs.org.

References

(1) Soderling, S. H.; Beavo, J. A. Regulation of cAMP and cGMP Signaling: New Phosphodiesterases and New Functions. *Curr. Opin. Cell Biol.* **2000**, *12*, 174−179.

(2) Beavo, J. A. Cyclic Nucleotide Phosphodiesterases: Functional Implications of Multiple Isoforms. *Physiol. Rev.* **1995**, *75*, 725−748.

(3) Mehats, C.; Andersen, C. B.; Filopanti, M.; Jin, S. L.; Conti, M. Cyclic Nucleotide Phosphodiesterases and Their Role in Endocrine Cell Signaling. *Trends Endocrinol. Metab.* **2002**, *13*, 29−35.

(4) Torphy, T. J. Phosphodiesterase Isozymes: Molecular Targets for Novel Antiasthma Agents. *Am. J. Respir. Crit. Care Med.* **1998**, *157*, 351−370.

(5) Corbin, J. D.; Francis, S. H. Cyclic GMP Phosphodiesterase-5: Target of Sildenafil. *J. Biol. Chem.* **1999**, *274*, 13729−13732.

(6) Card, G. L.; England, B. P.; Suzuki, Y.; Fong, D.; Powell, B.; Lee, B.; Luu, C.; Tabrizizad, M.; Gillette, S.; Ibrahim, P. N.; Artis, D. R.; Bollag, G.; Milburn, M. V.; Kim, S. H.; Schlessinger, J.; Zhang, K. Y. Structural Basis for the Activity of Drugs that Inhibit Phosphodiesterases. *Structure* **2004**, *12*, 2233−2247.

(7) Manallack, D. T.; Hughes, R. A.; Thompson, P. E. The Next Generation of Phosphodiesterase Inhibitors: Structural Clues to Ligand and Substrate Selectivity of Phosphodiesterases. *J. Med. Chem.* **2005**, *48*, 3449−3462.

(8) Zhang, K. Y.; Card, G. L.; Suzuki, Y.; Artis, D. R.; Fong, D.; Gillette, S.; Hsieh, D.; Neiman, J.; West, B. L.; Zhang, C.; Milburn, M. V.; Kim, S. H.; Schlessinger, J.; Bollag, G. A Glutamine Switch Mechanism for Nucleotide Selectivity by Phosphodiesterases. *Mol. Cell* **2004**, *15*, 279−286.

(9) Sung, B. J.; Hwang, K. Y.; Jeon, Y. H.; Lee, J. I.; Heo, Y. S.; Kim, J. H.; Moon, J.; Yoon, J. M.; Hyun, Y. L.; Kim, E.; Eum, S. J.; Park, S. Y.; Lee, J. O.; Lee, T. G.; Ro, S.; Cho, J. M. Structure of the Catalytic Domain of Human

Phosphodiesterase 5 with Bound Drug Molecules. *Nature* **2003**, *425*, 98−102.

(10) Corbin, J. D.; Beasley, A.; Blount, M. A.; Francis, S. H. Vardenafil: Structural Basis for Higher Potency over Sildenafil in Inhibiting cGMP-Specific Phosphodiesterase-5 (PDE5). *Neurochem. Int.* **2004**, *45*, 859−863.

(11) Liu, H.; Mark, A. E.; van Gunsteren, W. F. Estimating the Relative Free Energy of Different Molecular States with Respect to a Single Reference State. *J. Phys. Chem.* **1996**, *100*, 9485−9494.

(12) Pitera, J. W.; van Gunsteren, W. F. One-Step Perturbation Methods for Solvation Free Energies of Polar Solutes. *J. Phys. Chem. B* **2001**, *105*, 11264−11274.

(13) Oostenbrink, C.; van Gunsteren, W. F. Single-Step Perturbations to Calculate Free Energy Differences from Unphysical Reference States: Limits on Size, Flexibility, and Character. *J. Comput. Chem.* **2003**, *24*, 1730−1739.

(14) van Gunsteren, W. F.; Billeter, S. R.; Eising, A. A.; Hünenberger, P. H.; Krüger, P.; Mark, A. E.; Scott, W. R. P.; Tironi, I. G. *Biomolecular Simulation: The GROMOS96 Manual and User Guide*; Biomos: Zurich, Switzerland, 1996.

(15) Berendsen, H. J.; Postma, J. P.; van Gunsteren, W. F.; Hermans, J. *Intermolecular Forces*; Reidel: Dordrecht, The Netherlands, 1981; pp 331−342.

(16) Fiser, A.; Do, R. K.; Sali, A. Modeling of Loops in Protein Structures. *Protein Sci.* **2000**, *9*, 1753−1773.

(17) Fiser, A.; Sali, A. ModLoop: Automated Modeling of Loops in Protein Structures. *Bioinformatics* **2003**, *19*, 2500−2501.

(18) Berendsen, H. J. C.; Postma, J. P.; van Gunsteren, W. F.; DiNola, A.; Haak, J. R. Molecular Dynamics with Coupling to an External Bath. *J. Chem. Phys.* **1984**, *81*, 3684−3690.

(19) Schuler, L. D.; Daura, X.; van Gunsteren, W. F. An Improved GROMOS96 Force Field for Aliphatic Hydrocarbons in the Condensed Phase. *J. Comput. Chem.* **2001**, *22*, 1205−1218.

(20) Ryckaert, J. P.; Ciccotti, G.; Berendsen, H. J. C. Numerical-Integration of Cartesian Equations of Motion of a System with Constraints - Molecular Dynamics of n-Alkanes. *J. Comput. Phys.* **1977**, *23*, 327−341.

(21) van Gunsteren, W. F.; Beutler, T. C.; Fraternali, F.; King, P. M.; Mark, A. E.; Smith, P. E. *Computer Simulation of Biomolecular Systems, Theoretical and Experimental Applications*; ESCOM Science Publishers: Leiden, The Netherlands, 1993; pp 315−348.

(22) Beutler, T. C.; Mark, A. E.; van Schaik, R. C.; Gerber, P. R.; van Gunsteren, W. F. Avoiding Singularities and Numerical Instabilities in Free Energy Calculations Based on Molecular Simulations. *Chem. Phys. Lett.* **1994**, *222*, 529−539.

(23) Zacharias, M.; Straatsma, T. P.; McCammon, J. A. Separation-Shifted Scaling, a New Scaling Method for Lennard-Jones Interactions in Thermodynamic Integration. *J. Chem. Phys.* **1994**, *100*, 9025−9031.

(24) Allen, M. P.; Tildesley, D. J. *Computer Simulations of Liquids*; Oxford University Press Inc.: New York, 1989.

(25) Oostenbrink, B. C.; Pitera, J. W.; van Lipzig, M. M.; Meerman, J. H.; van Gunsteren, W. F. Simulations of the Estrogen Receptor Ligand-Binding Domain: Affinity of Natural Ligands and Xenoestrogens. *J. Med. Chem.* **2000**, *43*, 4594−4605.

(26) Oostenbrink, C.; van Gunsteren, W. F. Free Energies of Binding of Polychlorinated Biphenyls to the Estrogen Receptor from a Single Simulation. *Proteins* **2004**, *54*, 237−246.

(27) Oostenbrink, C.; van Gunsteren, W. F. Efficient Calculation of Many Stacking and Pairing Free Energies in DNA from a Few Molecular Dynamics Simulations. *Chem.—Eur. J.* **2005**, *11*, 4340−4348.

(28) Oostenbrink, C.; van Gunsteren, W. F. Free Energies of Ligand Binding for Structurally Diverse Compounds. *Proc. Natl. Acad. Sci. U.S.A.* **2005**, *102*, 6750−6754.

(29) Oostenbrink, C.; Soares, T. A.; van der Vegt, N. F.; van Gunsteren, W. F. Validation of the 53A6 GROMOS Force Field. *Eur. Biophys. J.* **2005**, *34*, 273−284.

(30) Zwanzig, R. W. High-Temperature Equation of State by a Perturbation Method. I. Nonpolar Gases. *J. Chem. Phys.* **1954**, *22*, 1420−1426.

(31) Ballard, S. A.; Gingell, C. J.; Tang, K.; Turner, L. A.; Price, M. E.; Naylor, A. M. Effects of Sildenafil on the Relaxation of Human Corpus Cavernosum Tissue in Vitro and on the Activities of Cyclic Nucleotide Phosphodiesterase Isozymes. *J. Urol.* **1998**, *159*, 2164−2171.

(32) Corbin, J. D.; Turko, I. V.; Beasley, A.; Francis, S. H. Phosphorylation of Phosphodiesterase-5 by Cyclic Nucleotide-Dependent Protein Kinase Alters Its Catalytic and Allosteric cGMP-Binding Activities. *Eur. J. Biochem.* **2000**, *267*, 2760−2767.

(33) Corbin, J. D.; Blount, M. A.; Weeks, J. L., II; Beasley, A.; Kuhn, K. P.; Ho, Y. S.; Saidi, L. F.; Hurley, J. H.; Kotera, J.; Francis, S. H. [3H]Sildenafil Binding to Phosphodiesterase-5 is Specific, Kinetically Heterogeneous, and Stimulated by cGMP. *Mol. Pharmacol.* **2003**, *63*, 1364−1372.

(34) Wang, H.; Liu, Y.; Huai, Q.; Cai, J.; Zoraghi, R.; Francis, S. H.; Corbin, J. D.; Robinson, H.; Xin, Z.; Lin, G.; Ke, H. Multiple Conformations of Phosphodiesterase-5: Implications for Enzyme Function and Drug Development. *J. Biol. Chem.* **2006**, *281*, 21469−21479.

CT600322D